International Journal of Nanomedicine

Dovepress
open access to scientific and medical research

Open Access Full Text Article

ORIGINAL RESEARCH

Exploration of alginate hydrogel/nano zinc oxide composite bandages for infected wounds

This article was published in the following Dove Press journal:
International Journal of Nanomedicine
1 October 2015
Number of times this article has been viewed

Annapoorna Mohandas*
Sudheesh Kumar PT*
Biswas Raja
Vinoth-Kumar Lakshmanan
Rangasamy Jayakumar

Amrita Centre for Nanosciences and Molecular Medicine, Amrita Institute of Medical Sciences and Research Centre, Amrita Vishwa Vidyapeetham University, Kochi, India

*These authors contributed equally to this work

Abstract: Alginate hydrogel/zinc oxide nanoparticles (nZnO) composite bandage was developed by freeze-dry method from the mixture of nZnO and alginate hydrogel. The developed composite bandage was porous with porosity at a range of 60%–70%. The swelling ratios of the bandages decreased with increasing concentrations of nZnO. The composite bandages with nZnO incorporation showed controlled degradation profile and faster blood clotting ability when compared to the KALTOSTAT® and control bandages without nZnO. The prepared composite bandages exhibited excellent antimicrobial activity against *Escherichia coli, Staphylococcus aureus, Candida albicans*, and methicillin resistant *S. aureus* (MRSA). Cytocompatibility evaluation of the prepared composite bandages done on human dermal fibroblast cells by Alamar assay and infiltration studies proved that the bandages have a non-toxic nature at lower concentrations of nZnO whereas slight reduction in viability was seen with increasing nZnO concentrations. The qualitative analysis of ex-vivo re-epithelialization on porcine skin revealed keratinocyte infiltration toward wound area for nZnO alginate bandages.

Keywords: alginate, hydrogel, ZnO nanoparticle, hemostatic, antimicrobial activity, wound healing

Introduction

Wound healing is a complex biological process which comprises blood coagulation, inflammation, proliferation, and remodeling.[1–4] The body replaces injured tissue by this complicated and dynamic process.[5] Under certain pathological conditions such as diabetes, microbial infection, or heavy blood loss, healing gets hampered.[6,7] Hence, it is important to treat the wound immediately with proper care.[8] Wound dressings are one of the major materials used for wound healing. Depending on the condition of the wound, the dressing material has to be selected.[9,10] An ideal wound dressing should be easily removable without causing trauma to the healed tissue, capable of absorbing exudates from the wound surface to prevent infection, and should be porous in order to allow the gaseous exchange between the atmosphere and wound surface.[11–15] The degradation products of the wound dressing materials can play a role in better wound healing.[16,17]

Commercially a lot of dressing materials are available made of synthetic and natural polymer based materials.[18,19] Synthetic polymer based dressings are mainly made of poly(urethane), poly(vinyl alcohol), poly(lactic acid), etc.[20–24] Natural polymers includes chitin, chitosan, gelatin, collagen, alginate, etc.[25–34] One of the drawbacks associated with synthetic polymer based dressing materials is their non-hemostatic nature and the degradation products being toxic.[19] Among the natural polymers, sodium alginate is a natural linear polysaccharide consisting of mannuronic acid and guluronic acid units.[35–41] Alginate proved to have biocompatibility, non-toxicity, non-immunogenicity,

Correspondence: R Jayakumar
Amrita Centre for Nanosciences and Molecular Medicine, Amrita Institute of Medical Sciences, Amrita Vishwa Vidhyapeetham, Kochi-682 041, India
Tel +91 484 280 1234
Fax +91 484 280 2020
Email rjayakumar@aims.amrita.edu

biodegradability, antimicrobial activity, and can be simply gelled with divalent cations. Even though enzymes in the human body lack the property to degrade alginate, the ionic compounds, especially calcium salts in the wound exudates, can cause swelling and subsequent degradation. The degradation rate also depends on the type of cross-linkers used.[42] Chitosan is easily prone to lysozymal attack. Apart from the hemostatic and antimicrobial activity, the degradation property of alginate could be enhanced with the incorporation of chitosan hydrogel. Literature reports the use of alginate gel based dressing materials for wound healing applications.[35–41]

A hydrogel based dressing material gives soothing effect to the wound surface by absorbing a large volume of exudate from the wound surface and this helps in prevention of infection. Hydrogel based materials can provide moist atmosphere at the wound site and can be easily peeled off when the wound is healed, which is essential for better wound healing.[35] In this work, we have developed and characterized alginate hydrogel/zinc oxide nanoparticles (nZnO) composite bandage. The incorporation of nZnO was done to impart antimicrobial activity to the developed composite bandage.[43] According to the reports, metallic nanoparticles have shown improved antimicrobial activity toward resistant strains with minimal toxicity to human cells.[26–28] Zinc ion based nanoparticles have broad potential to enhance wound healing.[43–45] nZnO has immense applications in the cosmetic industry, however there is a rising concern about the toxicity. Our previous studies with nZnO claim minimal toxicity to normal cells for particle sizes less than 100 nm.[46,47] There has been improved wound healing with reduced microbial flora in a full thickness wound healing model after application of nZnO containing bandages.[43,44]

Experiments

Materials

Alginate was purchased from Koyo Chemical Co Ltd, Osaka, Japan. Sodium hydroxide, zinc acetate dihydrate, and acetic acid were purchased from Qualigens, Mumbai, India. Hen lysozyme was purchased from Sigma-Aldrich Co., St Louis, MO, USA. DAPI (4′,6-diamidino-2-phenylindole), Alamar blue, Trypsin-EDTA (ethylenediaminetetraacetic acid) and fetal bovine serum (FBS) were obtained from Thermo Fisher Scientific, Waltham, MA, USA. Normal human dermal fibroblast (HDF) cells were purchased from Promocell, Heidelberg, Germany. Luria-Bertani broth (LB broth), Sabouraud Dextrose broth (SD broth) Agar-Agar, and Sabouraud Chloramphenicol Agar were purchased from Himedia, Mumbai, India.

Bacterial and fungal strains

Escherichia coli (American Type Culture Collection [ATCC] 25922, Manassas, VA, USA), *Staphylococcus aureus* (ATCC 25923), and methicillin resistant *S. aureus* (MRSA) strains were cultured in LB broth with 160 rpm shaking at 37°C. *Candida albicans* (ATCC 10231) was cultured in SD broth under similar conditions. MRSA strains which we have used from this study were originally isolated from patients' samples and provided to us by Microbiology Department, Amrita Institute of Medical Sciences, Kochi, India.

Preparation of alginate hydrogel/nZnO composite bandages

Alginate solution (3% w/w) was prepared by dissolving alginate powder in distilled water at room temperature. Chitosan hydrogel (1% w/w) was prepared by dissolving chitosan in 1% acetic acid followed by precipitation using 1% NaOH solution. The obtained mixture was centrifuged and the pellet was further washed to remove excess acetic acid. The obtained chitosan pellet was mixed with alginate solution (3% w/w) as a cross-linker to strengthen the alginate hydrogel. The mixture was stirred for 1 hour to obtain alginate hydrogel. The obtained alginate hydrogel was washed with deionized water to get rid of unwanted ions. nZnO was prepared as per the method reported earlier.[44] The precursors used were zinc acetate and sodium hydroxide. Methanol was used as the solvent. The solvents from the nanosuspension were removed by centrifugation at 20,000 rpm for 30 minutes. The obtained nZnO pellet was then resuspended in water and sonicated by probe sonicator for 10 minutes. The suspension thus formed was added into the alginate hydrogel at different concentrations (0.05% to 1% w/w) and stirred for 1 hour to get homogenous distribution. The slurry was then freeze-dried to obtain porous and flexible composite bandages.

Characterizations

The prepared alginate hydrogel/nZnO composite bandages were characterized using X-ray diffraction (XRD) (PANalytical X'Pert PRO, Cu Kα radiation, operating at a voltage of 40 kV). The structural morphology of alginate hydrogel/nZnO composite bandages was characterized by scanning electron microscopy (SEM) (JSM-6490LA; JEOL, Tokyo, Japan) after sputter coating the samples with gold. Figure 1 shows the photographical representation of alginate hydrogel/nZnO composite bandage preparation.

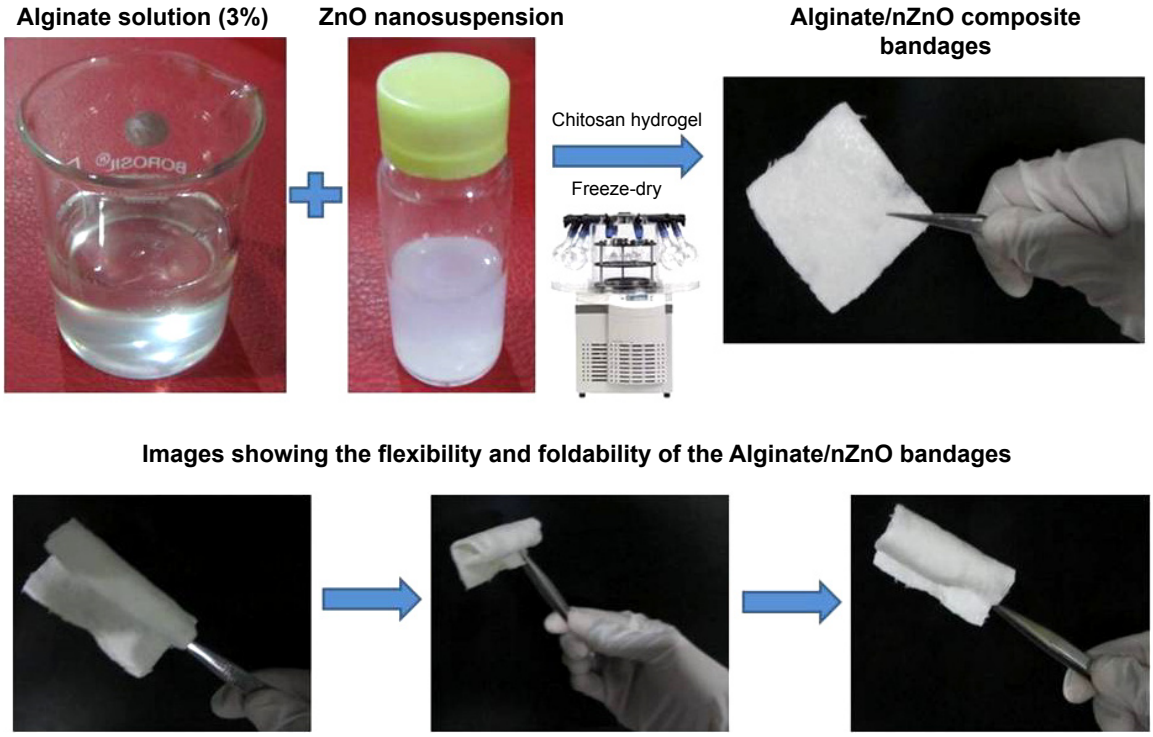

Figure 1 Photographical representation of the preparation of alginate hydrogel/zinc oxide nanoparticles (nZnO) composite bandages.

Porosity of alginate hydrogel/nZnO composite bandage

Porosity of the composite bandages was measured by alcohol displacement method.[27] Briefly, (10 mg, 1×1 mm) bandages were immersed in 1 mL ethanol, just enough to saturate the bandages. After 24 hours the materials were taken out and weighed. Porosity (P) was calculated by the formula:

$$P = (W_2 - W_1)/(\rho V_1) \quad (1)$$

where W_1 and W_2 indicates the weight of the bandages before and after immersing, respectively, and V_1 is the volume of alcohol before immersing, ρ is density of alcohol which is a constant.

Swelling ratio of alginate hydrogel/nZnO composite bandage

Bandage pieces of similar size and weight (10 mg, 1×1 mm) were immersed in phosphate buffered saline (PBS) of pH 7.4 at 37°C. The bandage pieces were taken out at pre-determined time intervals and weighed. Swelling ratio was calculated using the formula:

$$DS \text{ (degree of swelling)} = [(W_w - W_d)/W_d] \times 100 \quad (2)$$

where W_w is the wet weight and W_d is the dry weight of the bandage pieces.

In vitro biodegradation evaluation of alginate hydrogel/nZnO composite bandage

Bandages were weighed uniformly (10 mg, 1×1 mm) and immersed in lysozyme (10,000 U/mL) containing medium and incubated at 37°C for 21 days.[44,48] Initial weight of the bandage was noted as W_i. After 7, 14, and 21 days; each set of bandages was taken out from the PBS containing lysozyme, washed with deionized water to remove ions adsorbed on surface and freeze-dried. The dry weight was noted as W_t. The degradation of bandage was calculated using the formula:

$$\text{Degradation } (\%) = [(W_i - W_t)/W_i] \times 100 \quad (3)$$

Hemostatic potential of alginate hydrogel/nZnO composite bandage

Hemostatic potential of the bandages was assessed by the blood clotting analysis.[27] Blood clotting study was conducted as follows; human blood was collected from the ulnar vein from healthy volunteers (supplied from blood bank at Amrita

Institute of Medical Sciences) using sterile syringe mixed with anticoagulant acid citrate dextrose. Acid citrate dextrose-blood mixture (100 µL) was poured on the bandages and 5 µL of 0.2 M $CaCl_2$ was added to this to initiate the clotting. The samples (10 mg, 1×1 mm) were kept for incubation at 37°C for 20 minutes on a shaking incubator. Blood clotting was analyzed by measuring the optical density at 540 nm using a plate reader (BioTek PowerWave XS, Winooski, VT, USA).

In vitro antibacterial and antifungal activity evaluation

The antimicrobial activity was evaluated against Gram positive *S. aureus*, Gram negative *E. coli*, and fungal strain *C. albicans*. The bacterial strains were cultured in LB broth and fungal strain was cultured in SD broth respectively. The cultures were transferred to fresh and sterile plastic tubes containing corresponding broth at a concentration of 1×10^6 CFU/mL. The ethylene oxide sterilized bandage pieces (10 mg, 1×1 mm) were added to the tubes and kept for incubation at 37°C for 24 hours. After the specified time period, broth containing the bacteria and fungus were serially diluted in sterile saline and plated on LB agar and Sabouraud Chloramphenicol Agar (SCA) plates respectively.[26, 27]

Antibacterial activity against MRSA was evaluated by disk diffusion method.[27] The bacterial strain was isolated from a patient and cultured in LB broth. The MRSA culture was streaked on an LB agar plate and the composite bandage in the form of a 13 mm diameter disk was kept on the surface of the LB agar plate. The plate was kept for incubation overnight. The zone of inhibition was noted to determine the antibacterial effect of the composite bandage against MRSA.

Evaluation of membrane potential of bacteria

S. aureus and *E. coli* were grown in LB broth at 37°C. Bacterial cells from the mid-exponential phase cultures were centrifuged and the pellet was re-suspended in PBS, pH 7.4 at room temperature at an optical density of 0.3–0.5 at 610 nm. Composite bandages (10 mg, 1×1 mm) were added to the *S. aureus* and *E. coli* suspension, and incubated for 1 hour, followed by the addition of 10 µL of 3 mM DiOC2 (diethyloxacarbocyanine) and 2 µL of Triton X-100. The samples were incubated at room temperature for 5 minutes and the relative green fluorescence was measured at excitation/emission 480 nm/520 nm and red fluorescence at 480 nm/620 nm. Cells treated with DiOC2 alone served as a positive control while cells treated with both DiOC2 and Triton X-100 served as negative control.

Cell viability evaluation

Alamar blue assay method was used to assess the cell viability of the composite bandages.[44] Briefly, the bandage pieces (10 mg, 1×1 mm) which were sterilized by ethylene oxide gas were added to 12-well cell culture plates. HDF cells were trypsinized after reaching confluency of 80% and seeded onto the bandage pieces immersed in cell culture medium at a density of 5,000 cells per well. The bandages were then kept for incubation up to 72 hours and then culture medium was removed and Alamar blue was added at specified time intervals. After the incubation period the viability was measured by reading the optical density at 570 nm with 620 nm set as the reference wavelength using a microplate spectrophotometer (BioTek PowerWave XS).

Cell attachment and DAPI staining

HDF cells were seeded on the composite bandages at a density of 1×10^4 cells and kept for 24 hours of incubation. After the incubation time, the bandages were washed with PBS and fixed with 1% glutaraldehyde solution for 1 hour. The samples were thoroughly washed with PBS and dehydrated in a graded ethanol series, air-dried, gold sputtered in vacuum, and examined with SEM.

The cell seeded bandages were fixed with 4% paraformaldehyde for 20 minutes, permeabilized with 0.5% Triton X-100 (in PBS) for 5 minutes. Then the bandages were treated with 1% FBS, washed with PBS and stained with 50 µL of DAPI and incubated in the dark for 3 minutes. The bandages were then washed with PBS and viewed under fluorescent microscope (Olympus-BX-51).

Cell infiltration analysis of alginate hydrogel/nZnO composite bandage

HDF cells were seeded at a density of 10,000 cells onto the bandage pieces and cultured for 48 hours. After incubation, the culture medium was discarded and washed with PBS. The cells were fixed with 4% paraformaldehyde for 15 minutes and washed with PBS. The cell permeabilization and blocking steps were carried out using 0.5% Triton for 10 minutes and 1% bovine serum albumin for 20 minutes respectively. The samples were incubated in the dark with tetramethylrhodamine (TRITC) conjugated phalloidin for 1 hour. Images were taken by laser confocal microscope.

Ex vivo re-epithelialization study of composite bandages

Wound was made on porcine ear skin using 3 mm diameter biopsy punch. The excised skin was rinsed in PBS.

The samples (10 mg, 1×1 mm) were placed in keratinocyte growth media with 10% FBS and antibiotic antimycotic followed by incubation with alginate control and alginate hydrogel/nZnO composite bandage for 48 hours in a sterile incubator supplying 5% CO_2. The skin samples were embedded in tissue freezing medium followed by sectioning of 5 µm thickness using a cryotome. The sections were mounted on poly-l-lysine-coated glass slides and further stained using hematoxylin and eosin. Samples were taken in triplicates.

Statistical analysis

The values obtained from the experiments were expressed as means ± standard deviation. Statistical significance for all the experiments was determined by Student's *t*-test and the data were considered significant for *P*-values <0.05.

Results and discussion

Characterization

In this work we have developed and characterized alginate bandages after incorporation of nZnO. As previously reported nZnO were in the size range of 70–120 nm. Figure 2A shows the SEM images of alginate hydrogel/nZnO composite bandages. The bandages were micro-porous with interconnected pores in the size range of 200–400 µm. Figure 2B represents the XRD spectra of alginate hydrogel/nZnO composite bandages. XRD spectra indicated an amorphous spectrum for alginate control. The characteristic peaks of nZnO at 31.6, 34.3, 36.2, 56.5, 62.8, and 67.8° were present in the spectra. The intensity of the peaks of nZnO increased with the increase in the concentration of nZnO.[43,44] Figure 2C shows the homogeneity in the distribution of nZnO on the bandages.[43]

Fourier transform infrared spectroscopy (FTIR) data of the alginate have been compared with the alginate + nZnO bandages. Both the bandages had the characteristic peak at 1,026, 1,409, and 1,593 cm^{-1} respectively (Figure 3). The peaks at this range is contributed by amine group in chitosan and carbonyl groups present in both chitosan and alginate. The control bandage had a peak at 3,565 (OH-group of alginate or chitosan) which got reduced to 3,265 for alginate nZnO. This broadening could be due to intermolecular hydrogen bonding between nZnO and alginate hydrogel.

Porosity, swelling ratio, and biodegradation of alginate hydrogel/nZnO composite bandage

Porosity was determined by alcohol displacement method. Porosity of alginate control bandages was ~60%–80% of the total bandage volume whereas nZnO incorporated composite bandages showed porosity of ~60%–70%. The reduction in porosity for the samples was not significant when compared to the alginate control. The decrease in porosity was due to the interaction of alginate with nZnO (Figure 4A). Ethanol is taken as a solvent since it does not dissolve lyophilized form of alginate or chitosan bandages. Porosity is largely influenced by pore size of a bandage and determines how well the material can absorb wound exudates or transport nutrients and oxygen. The fluid absorption would be helpful in controlling infection at the wound site.[5]

The swelling ratio for control bandage was 20 and the presence of nZnO slightly reduced the swelling ratio to 16–20 (Figure 4B). With increase in weight percentage up to 0.5%, the swelling ratio decreased significantly for nZnO incorporated alginate bandages. The swelling ratio of control bandage was slightly increased after 1 week when compared to the composite bandages. The reason might be due to the interaction of carboxylic acid functional groups of alginate with the hydrophilic medium.[48] After 2 weeks, the bandages showed no change in the swelling ratio. This might be due to the saturation of bandages with buffer. An infectious wound contains numerous exudates and slough which is largely determined by swelling ratio of bandages.

The presence of nZnO did not alter the degradation nature of the composite bandages (Figure 4C). All the bandages degraded 10%–15% after 1 week of immersion in PBS containing lysozyme. The degradation rate was further increased to 25%–30% after 2 weeks and 30%–40% after 3 weeks. The interaction between nZnO and alginate hydrogel might be weak. Hence the degradation profile was not changed. Chronic wounds, especially diabetic wounds are characterized by the presence of proteases of which lysozyme is the one that can degrade chitosan. Lysozyme specifically degrades β-1,4-glycosidic linkages between *N*-acetyl glucosamine and glucosamine in chitosan. However, alginate is being degraded by calcium ions in the PBS. This could be compared to wound fluid where there is an excess salt that makes degradation process easier.[48]

Hemostatic potential of alginate hydrogel/nZnO composite bandages

A lower optical density value at 540 nm indicates lower release of free hemoglobin from red blood cell (RBC) membrane lysis (Figure 5). Hence the increased blood clotting. All the nZnO incorporated alginate bandages had significant blood clotting when compared to the commercial KALTOSTAT® (Convatec, Greensboro, NC, USA) and blank bandages irrespective of

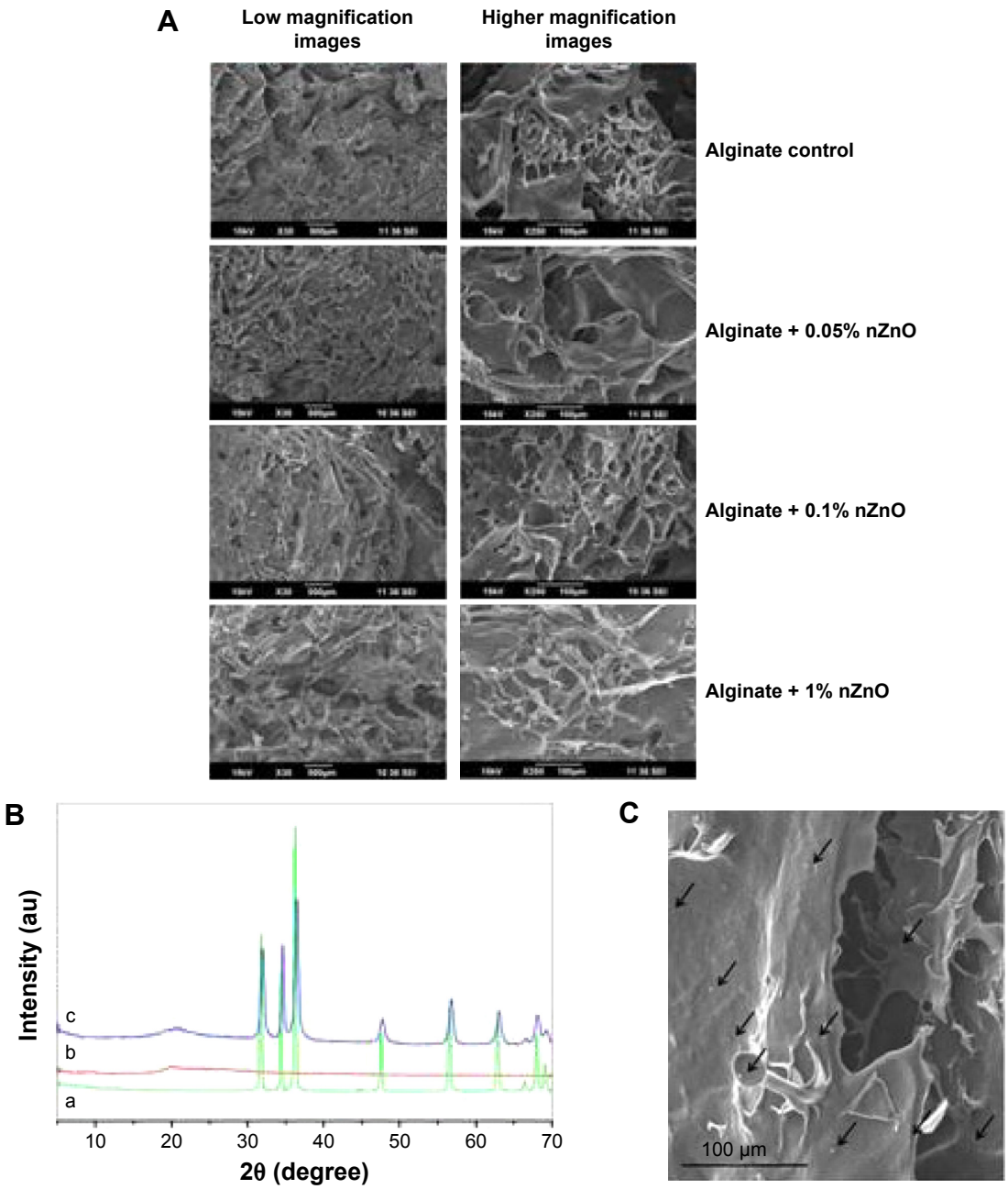

Figure 2 Physico-chemical charecterisation of alginate hydrogel/nZnO composite bandages.
Notes: (**A**) SEM images of alginate hydrogel/nZnO composite bandages. (**B**) XRD spectra of (a) nZnO control, (b) alginate control, and (c) alginate + nZnO composite bandage. (**C**) SEM image of alginate + nZnO composite bandage showing nZnO.
Abbreviations: SEM, scanning electron microscopy; XRD, X-ray diffraction; nZnO, zinc oxide nanoparticles.

nZnO concentrations. The presence of nZnO did not alter the hemostatic nature of alginate. Chitosan is known to activate blood clotting by releasing PDGF-AB and TGF-β1 from platelets that ultimately causes its aggregation toward blood clotting pathway.[49] KALTOSTAT® being an alginate based bandage would have assisted in blood clotting. Even though infectious wounds are devoid of heavy blood loss, certain wounds show moderate bleeding nature. The blood clotting nature of the bandage would be advantageous for bleeding wounds.

In vitro antibacterial and antifungal activity of alginate hydrogel/nZnO composite bandages

The antibacterial activity of the prepared composite bandages against *S. aureus* (Figure 6A) and *E. coli* (Figure 6B) was studied. In the figure, top to bottom indicates serial dilution of bacteria and left to right shows different samples. It is clear from the data that the number of bacterial colonies decreased in the presence of bandages with higher concentrations of

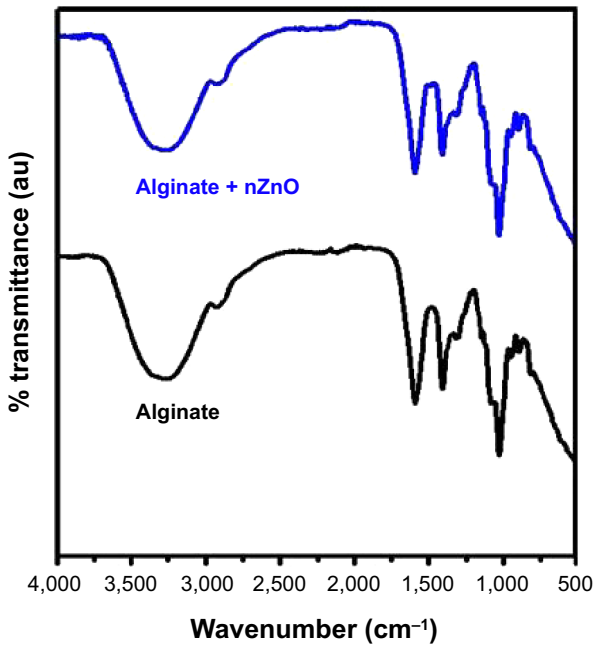

Figure 3 FTIR image of alginate control and alginate + nZnO bandages.
Abbreviations: FTIR, Fourier transform infrared spectroscopy; nZnO, zinc oxide nanoparticles; au, arbitrary units.

nZnO (0.75% and 1%). At lower concentrations of nZnO, the antibacterial activity was reduced and this might be due to the lower amount of release of nZnO from the bandages than the minimal effective concentration. The antibacterial activity of the prepared bandages showed similar results against both *S. aureus* and *E. coli*. The colonies were higher in control alginate bandage and KALTOSTAT®. The reduction in bacterial colonies was due to the interaction of nZnO with the bacteria.

Antifungal activity evaluation done against *C. albicans* (Figure 6C) proved the toxicity of the prepared composite bandages toward fungus. The number of viable fungal colonies was found to be decreased in the presence of bandages with higher concentrations of nZnO. The number of colonies was more when the concentration of nZnO was lower. However, alginate control and KALTOSTAT® exhibited less activity against candida than the nZnO incorporated ones. The cationic zinc ions would have caused the hyperpolarization of negatively charged membrane of candida causing it to burst, subsequently killing it.[50]

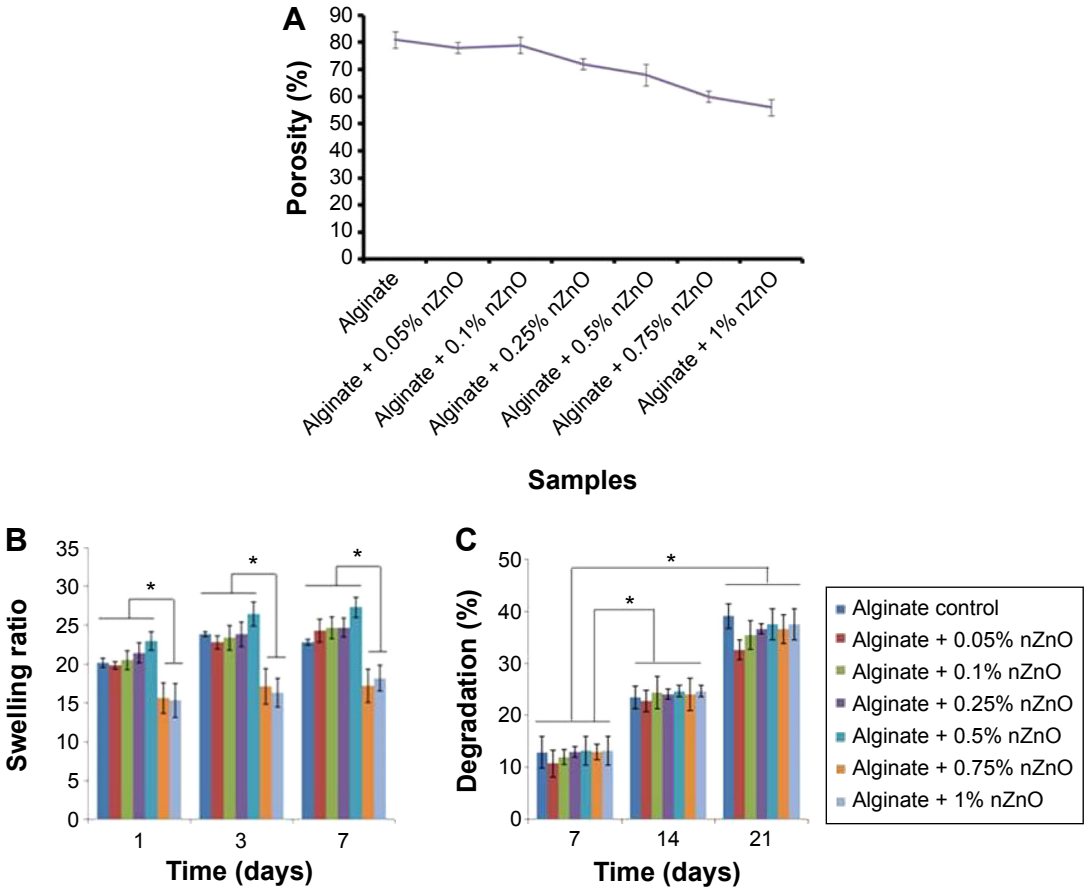

Figure 4 Biochemical properties of alginate hydrogel/nZno composite bandages.
Notes: (**A**) Porosity, (**B**) swelling ratio, and (**C**) biodegradation of alginate hydrogel/nZnO composite bandages compared with control alginate bandage. Student's *t*-test was performed and *P*-values <0.05 were considered significant. *Statistical significance of different bandages at each time point.
Abbreviation: nZnO, zinc oxide nanoparticles.

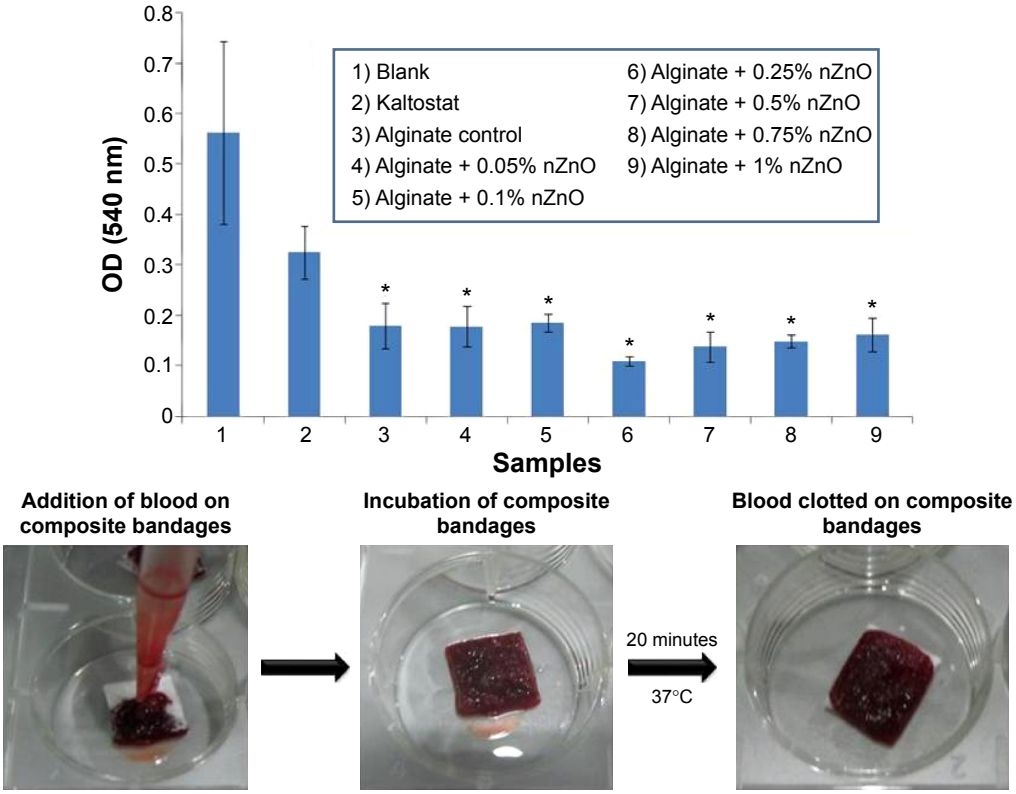

Figure 5 Blood clotting ability evaluation of alginate hydrogel/nZnO composite bandages with different concentrations of nZnO.
Note: Student's *t*-test was performed and *P*-values <0.05 were considered significant. *Indicates significant difference compared the control.
Abbreviations: nZnO, zinc oxide nanoparticles; OD, optical density.

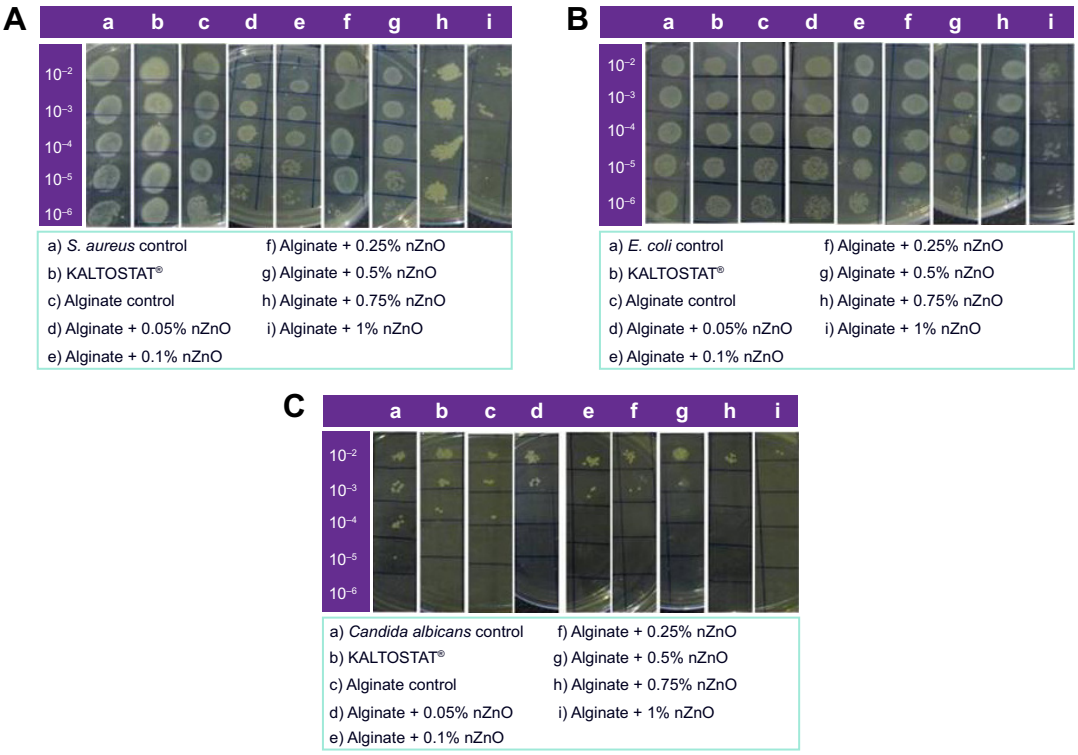

Figure 6 Antibacterial activity evaluation of alginate hydrogel/nZnO composite bandages.
Notes: Against (**A**) *Staphylococcus aureus* (*S. aureus*), (**B**) *Escherichia coli* (*E. coli*), and antifungal activity evaluation against (**C**) *Candida albicans* by serial dilution method. The label on y-axis shows dilution factor.
Abbreviation: nZnO, zinc oxide nanoparticles.

Antibacterial activity against MRSA of alginate hydrogel/nZnO composite bandage

Further, antibacterial activity was evaluated against two MRSA strains (Figure 7A). Composite bandages with 5% and 7.5% nZnO showed activity against these strains. There might be the formation of excess staphyloxanthin in MRSA that could contribute to the resistance of bacterial cells toward lower concentrations of nZnO.[51] Due to this reason the bandages with lower concentrations of nZnO did not show any activity against the tested strains.

The antimicrobial activity was due to the generation of ROS by the released zinc ions from the composite bandages. The generated ROS, due to the action of zinc ions, would have caused microbial cell wall damage and eventual death of the organism.[44,45]

Membrane potential evaluation of alginate hydrogel/nZnO composite bandages

Figure 7B represents the membrane potential evaluation data of *S. aureus* and *E. coli*. The composite bandages changed the membrane potential of tested bacterial strains and that caused depolarization, possibly leading to the bacterial cell disruption. The zinc ions released from the composite bandages might have changed the membrane potential of the bacterial cell wall and caused bacterial cell death.[45]

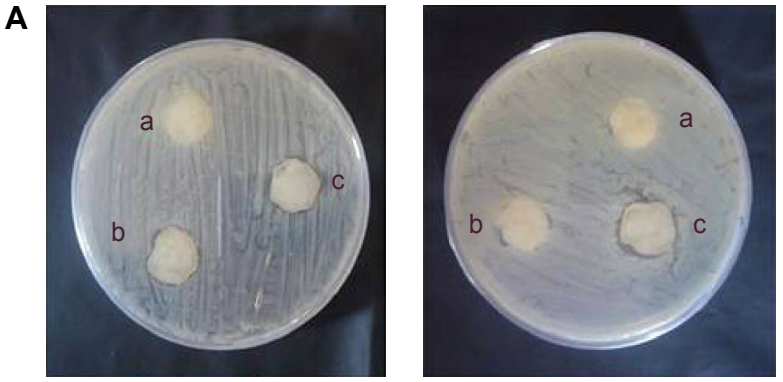

Sample	Strain 1	Strain 2
a	No zone	No zone
b	15±2 mm	14±1 mm
c	16±1 mm	18±2 mm

a) Alginate control b) Alginate + 5% nZnO (w/w) c) Alginate + 7.5% nZnO (w/w)

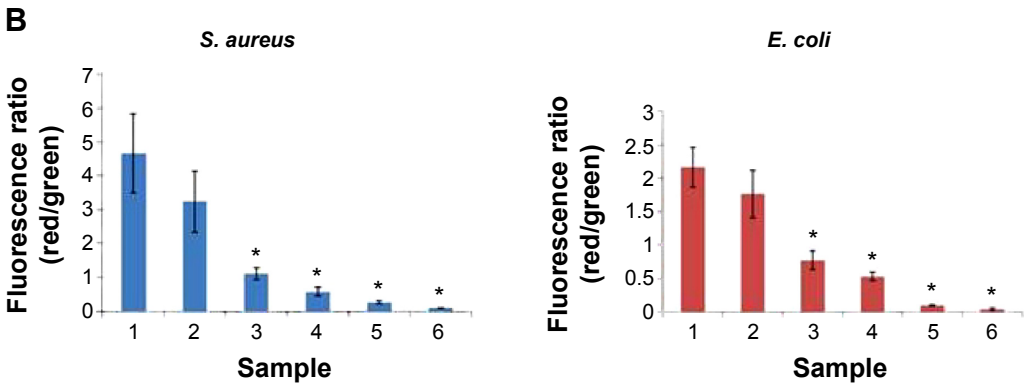

Figure 7 Evaluation of antibacterial activity of alginate hydrogel/nZnO composite bandages.
Notes: (**A**) Antibacterial activity evaluation of alginate hydrogel/nZnO composite bandages against MRSA by disk diffusion method. (**B**) Membrane potential evaluation of composite bandages. Student's *t*-test was performed and *P*-values <0.05 were considered significant. *Indicates significant difference compared the control.
Abbreviations: nZnO, zinc oxide nanoparticles; MRSA, methicillin resistant *Staphylococcus aureus*; *S. aureus*, *Staphylococcus aureus*; *E. coli*, *Escherichia coli.*

Cell viability evaluation

Cell viability of the prepared composite bandages was checked in the presence of HDF cells (Figure 8A). After 24 hours of incubation, bandages with higher concentrations of nZnO (0.25% to 1%) showed 40%–60% cell viability. Bandages with 0.05%, 0.1% of nZnO showed 90% viability after 24 hours of incubation. The viability remains unchanged after 48 and 72 hours. The decrease in the viability was due to the toxic effect of nZnO to the HDF cells. This might be due to the generation of ROS in the presence of nZnO which caused toxicity to the cells.[44,45]

Cell attachment, DAPI staining, and phalloidin staining

DAPI stained images revealed that the number of cells were higher in control bandage and bandages with lower concentrations of nZnO (Figure 8B and C). Figure 9Aa–f represents the laser confocal images of phalloidin stained bandages and merged images. The data showed that the number of HDF cells attached on the control bandage was more when compared to the composite bandages. HDF cell attachment, infiltration, and proliferation were assessed by SEM images of the bandages with the cells

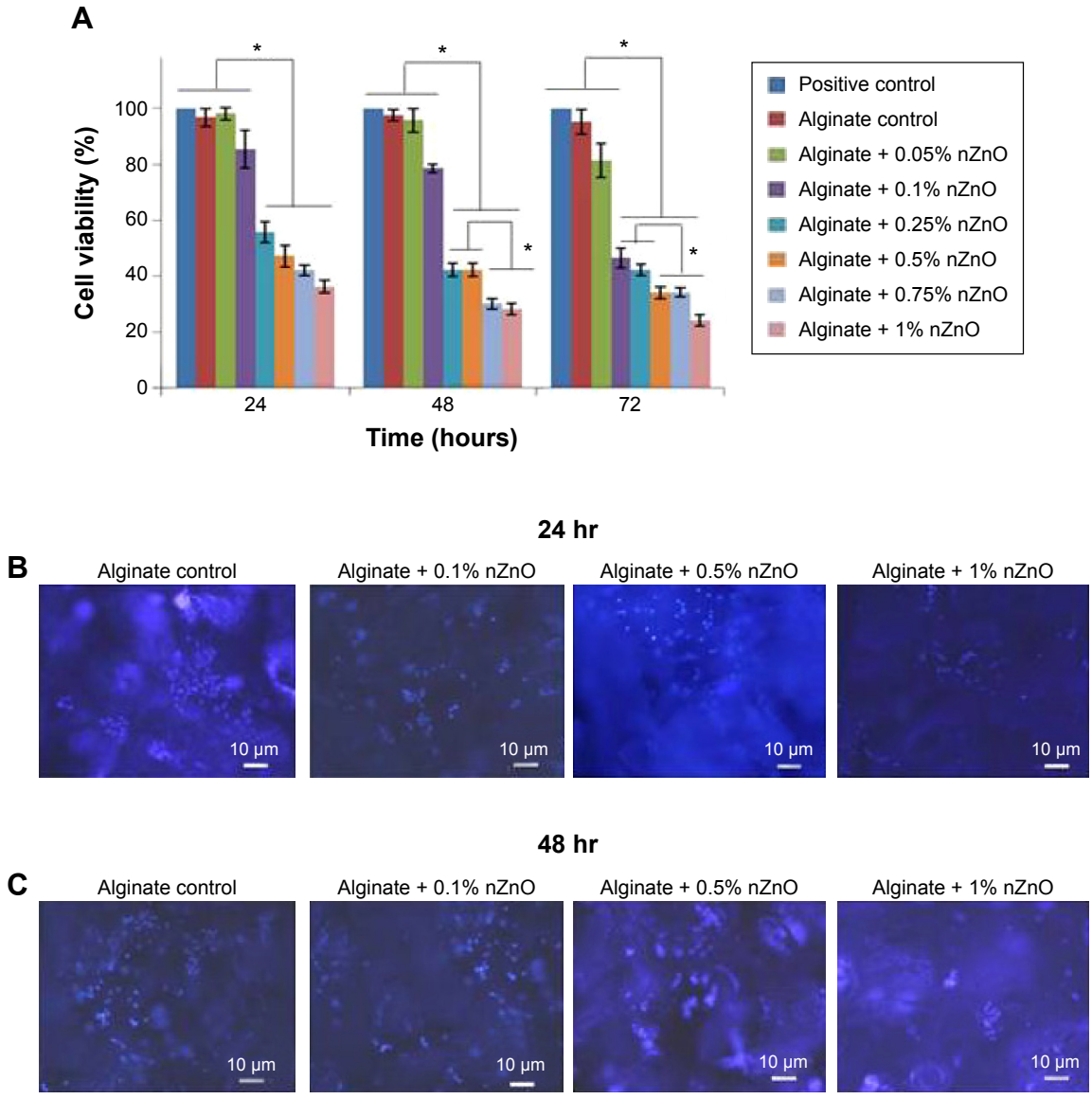

Figure 8 Evaluation of cytocompatability of alginate hydrogel/nZnO composite bandages.
Notes: (**A**) Cell viability evaluation of HDF cells using Alamar blue assay. Student's *t*-test was performed and *P*-values <0.05 were considered significant. (**B** and **C**) DAPI stained fluorescence microscopic images of HDF cells attached onto the composite bandages. *Indicates significant difference compared the control. Scale bar denotes 10 µm.
Abbreviations: HDF, human dermal fibroblast; DAPI, 4′,6-diamidino-2-phenylindole; nZnO, zinc oxide nanoparticles; hr, hours.

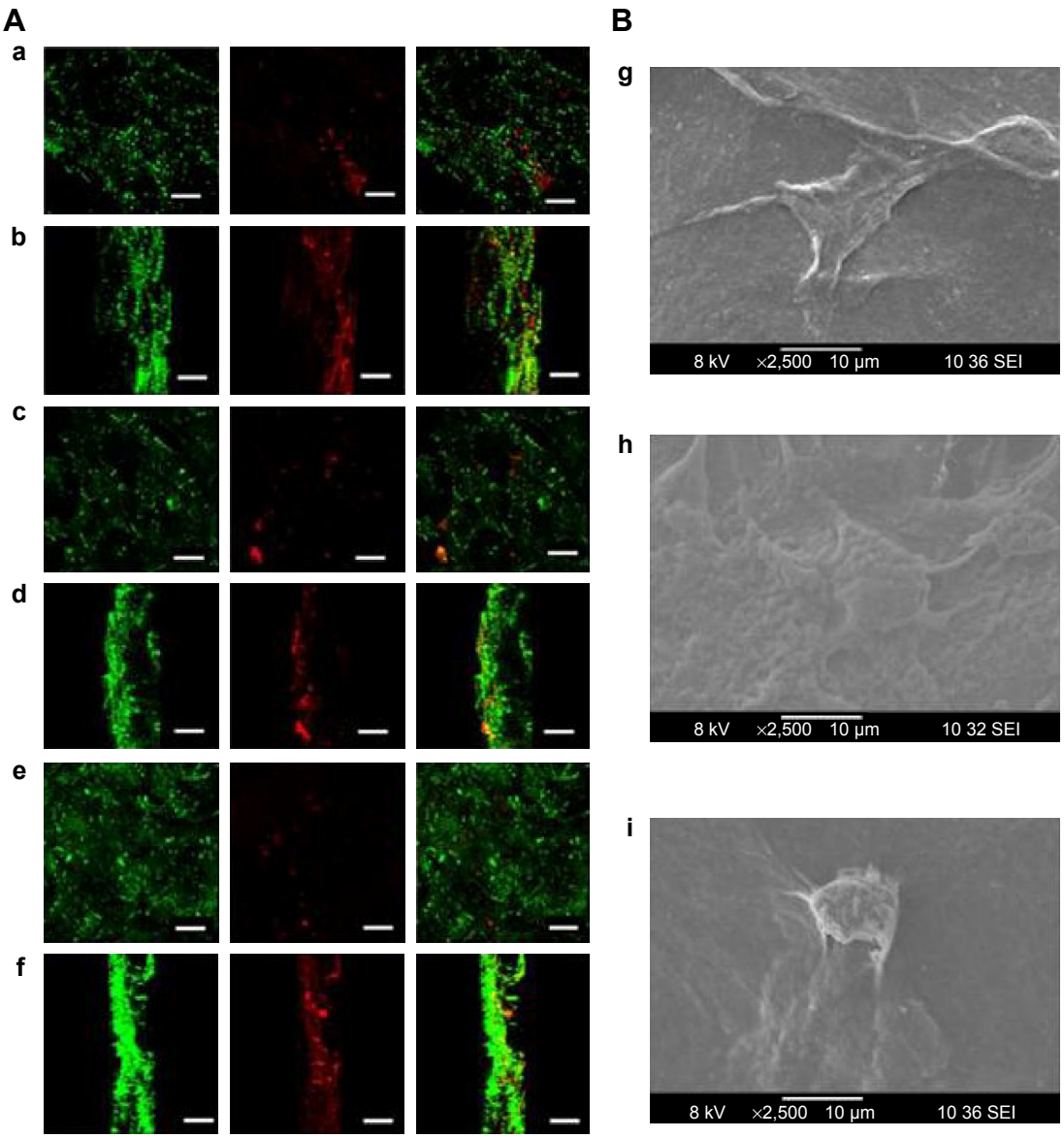

Figure 9 Qualitative cytocompatibilty evaluation of alginate hydrogel/nZnO composite bandages.
Notes: (**A**) Laser confocal images of phalloidin dye stained HDF cells attached and infiltrated into the composite bandages. (a and b) surface view and Z-stacked images of alginate control. (c and d) surface view and Z-stacked images of alginate + 0.01% nZnO. (e and f) surface view and Z-stacked images of alginate + 0.1% nZnO. Green color represents auto fluorescence image of scaffold whereas red fluorescence is phalloidin-TRITC dye. Scale bar denotes 100 µm. (**B**) SEM images of HDF cell attachment on (g) alginate control, (h) alginate + 0.01% nZnO, and (i) alginate + 0.1% nZnO.
Abbreviations: HDF, human dermal fibroblast; nZnO, zinc oxide nanoparticles; SEM, scanning electron microscopy; TRITC, tetramethylrhodamine.

(Figure 9Bg, h, and i). Confocal data show green color auto fluorescence of bandages whereas, red color is due to TRITC phalloidin stain of actin filaments. SEM images showed that there was a higher number of cells on the surface of control than on the surface of nZnO containing bandages. The presence of nZnO reduced the attachment of HDF cells on the composite bandages. The attached cells started proliferating on the bandage. The obtained data indicate that the bandages were capable of attracting cells onto it which is advantageous when the bandages are to be tested for preclinical and clinical trials.

Ex vivo re-epithelialization study of composite bandages

Epithelialization is favored by keratinocyte proliferation and migration toward the wounded area.[52,53] The re-epithelialization (marked with arrows) after 48 hours is shown with dashed lines (Figure 10A and B). The wound

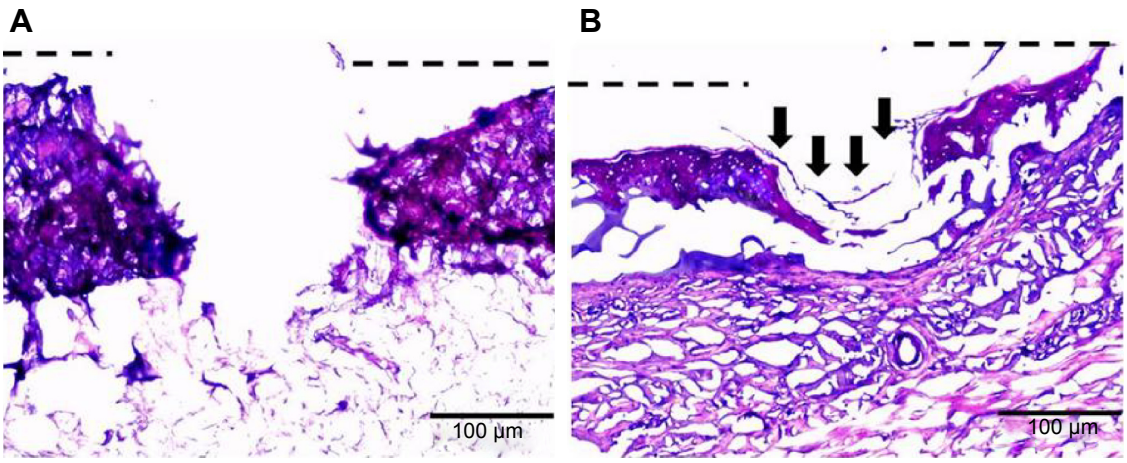

Figure 10 Hematoxylin and eosin stained images of ex vivo partial thickness wound model in porcine ear skin.
Notes: (**A**) Alginate control and (**B**) alginate hydrogel/nZnO (1%) composite bandages. Arrows indicate the re-epithelialization.
Abbreviation: nZnO, zinc oxide nanoparticles.

edges were being covered with epithelial cells both in alginate control and alginate/ZnO composite bandages. However, the effect is higher for alginate/ZnO composite bandages. This may be due to the release of zinc ions into the media, which would enhance the proliferation and migration of keratinocyte cells to the wounded area. It is known that the zinc ions activate MAPK pathway which helps in prevention of apoptosis.[53,54]

Conclusion

Alginate hydrogel/nZnO composite bandage was prepared by freeze-dry process. The prepared bandages were flexible. Porosity of the bandages was well within the range 60%–70% which is advantageous for a wound dressing. Porous nature of the bandages was not altered significantly after the addition of nZnO. Controlled biodegradation profile of the composite bandages would be helpful for faster healing of wounds. Hemostatic potential nature of the composite bandage extends its application potential to heavily bleeding wounds. The composite bandages showed significant antibacterial activity against a number of tested microbes including MRSA. This data revealed the potential of the material for infected wounds. HDF cell viability of the composite bandage was found to be dependent on the nZnO concentration. The cytocompatibility of the bandages was inversely proportional to the nZnO concentration. The bandages with lower concentration of nZnO showed no reduction in cell viability whereas bandages with higher concentration of nZnO exhibited slight toxicity. However, further wound healing evaluation of the prepared composite bandages has to be done for further understanding of the in vivo toxicity and wound healing mechanism.

Acknowledgments

The authors acknowledge Department of Biotechnology (DBT), India, for the financial support under a grant (BT/PR13885/MED/32/145/2010 dated January 3, 2011). We are also thankful to Nanomission, Department of Science and Technology, India, which supported this work, under a grant of the Nanoscience and Nanotechnology Initiative program. Raja Biswas is grateful to Ramalingaswami Fellowship, Department of Biotechnology, India, for the financial support. Annapoorna Mohandas is thankful to University Grant Commission, India for the Fellowship (Award No 20-12/2009 (ii) EU-IV dated July 31, 2010 SR No 2120930570). We are also grateful to Mr Sajin P Ravi and Mr Sarath KS for his help in SEM analysis and confocal analysis respectively. We are indebted to Amrita Centre for Nanosciences and Molecular Medicine for providing the infrastructure to complete this study.

Disclosure

The authors have no conflicts of interest to disclose.

References

1. Kiwanuka E, Junker J, Eriksson E. Harnessing growth factors to influence wound healing. *Clin Plast Surg*. 2012;39(3):239–248.
2. Ben Amar M, Wu M. Re-epithelialization: Advancing epithelium frontier during wound healing. *J R Soc Interface.* 2014;11(93):20131038.
3. Harishkumar M, Masatoshi Y, Hiroshi S, Tsuyomu I, Masugi M. Revealing the mechanism of in vitro wound healing properties of citrus tamurana extract. *Biomed Res Int*. 2013;2013:963457.
4. Ninan N, Muthiah M, Park IK, et al. Faujasites incorporated tissue engineering scaffolds for wound healing: in vitro and in vivo analysis. *ACS Appl Mater Interfaces.* 2013;5(21):11194–11206.
5. Jayakumar R, Prabaharan M, Kumar PT, Nair SV, Tamura H. Biomaterials based on chitin and chitosan in wound dressing applications. *Biotechnol Adv.* 2011;29(3):322–337.

6. Daeschlein G. Antimicrobial and antiseptic strategies in wound management. *Int Wound J.* 2013;10 Suppl 1:9–14.
7. Sofokleous P, Stride E, Edirisinghe M. Preparation, characterization, and release of amoxicillin from electrospun fibrous wound dressing patches. *Pharm Res.* 2013;30(7):1926–1938.
8. Dong Y, Hassan WU, Kennedy R, et al. Performance of an in situ formed bioactive hydrogel dressing from a PEG-based hyperbranched multifunctional copolymer. *Acta Biomater*. 2014;10(5): 2076–2085.
9. Mogoşanu GD, Grumezescu AM. Natural and synthetic polymers for wounds and burns dressing. *Int J Pharm*. 2014;463(2):127–136.
10. Kanokpanont S, Damrongsakkul S, Ratanavaraporn J, Aramwit P. An innovative bi-layered wound dressing made of silk and gelatin for accelerated wound healing. *Int J Pharm*. 2012;436(1–2):141–153.
11. Ji F, Lin W, Wang Z, et al. Development of nonstick and drug-loaded wound dressing based on the hydrolytic hydrophobic poly(carboxybetaine) ester analogue. *ACS Appl Mater Interfaces*. 2013; 5(21):10489–10494.
12. Broussard KC, Powers JG. Wound dressings: selecting the most appropriate type. *Am J Clin Dermatol*. 2013;14(6):449–459.
13. Abdelrahman T, Newton H. Wound dressings: principles and practice. *Surgery*. 2011;29(10):491–495.
14. Costache MC, Qu H, Ducheyne P, Devore DI. Polymer-xerogel composites for controlled release wound dressings. *Biomaterials*. 2010;31(24):6336–6343.
15. Rossi S, Faccendini A, Bonferoni MC, et al. Sponge-like dressings based on biopolymers for the delivery of platelet lysate to skin chronic wounds. *Int J Pharm*. 2013;440(2):207–215.
16. Elsner JJ, Egozi D, Ullmann Y, et al. Novel biodegradable composite wound dressings with controlled release of antibiotics: Results in a guinea pig burn model. *Burns*. 2011;37(5):896–904.
17. Fonder MA, Lazarus GS, Cowan DA, et al. Treating the chronic wound: A practical approach to the care of non healing wounds and wound care dressings. *J Am Acad Dermatol.* 2008;58(2):185–206.
18. Silva R, Ferreira H, Matamá T, Gomes AC, Cavaco-Paulo A. Wound-healing evaluation of entrapped active agents into protein microspheres over cellulosic gauzes. *Biotechnol J*. 2012;7(11):1376–1385.
19. Jones V, Grey JE, Harding KG. Wound dressings. *BMJ*. 2006;332(7544): 777–780.
20. Unnithan AR, Barakat NA, Pichiah PB, et al. Wound-dressing materials with antibacterial activity from electrospun polyurethane-dextran nanofiber mats containing ciprofloxacin HCl. *Carbohydr Polym*. 2012;90(4):1786–1793.
21. Lalit V. Role of natural polysaccharides in radiation formation of PVA–hydrogel wound dressing. *Nuclear Instruments and Methods in Physics Research*. 2007;255(2):343–349.
22. Kokabi M, Sirousazar M, Hassan ZM. PVA-clay nanocomposite hydrogels for wound dressing. *Eur Polym J*. 2007;43(3):773–781.
23. Pandey A, Pandey GC, Aswath PB. Synthesis of polylactic acid-polyglycolic acid blends using microwave radiation. *J Mech Behav Biomed*. 2008;1(3):227–233.
24. Aoki S, Kinoshita M, Miyazaki H, et al. Application of poly-L-lactic acid nanosheet as a material for wound dressing. *Plast Reconstr Surg*. 2013;131(2):236–240.
25. Pechter PM, Gil J, Valdes J, et al. Keratin dressings speed epithelialization of deep partial-thickness wounds. *Wound Repair Regen*. 2012; 20(2):236–242.
26. Sohnle PG, Collins- Lech C, Wiessner JH. The Zinc-Reversible Antimicrobial Activity of Neutrophil Lysates and Abscess Fluid Supernatants. *J Infect Dis.* 1991;164(1):137–142.
27. Sudheesh Kumar PT, Abhilash S, Manzoor K, Nair SV, Tamura H, Jayakumar R. Preparation and characterization of novel β-chitin/nano silver composite scaffolds for wound dressing applications. *Carbohydr Polym*. 2010;80(3):761–767.
28. Anisha BS, Biswas R, Chennazhi KP, Jayakumar R. Chitosan-hyaluronic acid/nano silver composite sponges for drug resistant bacteria infected diabetic wounds. *Int J Biol Macromol*. 2013;62:310–320.
29. Jayakumar R, Prabaharan M, Nair SV, Tamura H. Novel chitin and chitosan nanofibers in biomedical applications. *Biotechnol Adv*. 2010; 28(1):142–150.
30. Jayakumar R, Menon D, Manzoor K, et al. Biomedical applications of chitin and chitosan based nanomaterials-a short review. *Carbohydr Polym.* 2010;82(2):227–232.
31. Wang T, Zhu XK, Xue XT, Wu DY. Hydrogel sheets of chitosan, honey and gelatin as burn wound dressings. *Carbohydr Polym.* 2012;88(1): 75–83.
32. Azad AK, Sermsintham N, Chandrkrachang S, Stevens WF. Chitosan membrane as a wound-healing dressing: characterization and clinical application. *J Biomed Mater Res B Appl Biomater.* 2004;69(2): 216–222.
33. Adhirajan N, Shanmugasundaram N, Shanmuganathan S, Babu M. Collagen-based wound dressing for doxycycline delivery: in-vivo evaluation in an infected excisional wound model in rats. *J Pharm Pharmacol*. 2009;61(12):1617–1623.
34. Zhao R, Li X, Sun B, et al. Electrospun chitosan/sericin composite nanofibers with antibacterial property as potential wound dressings. *Int J Biol Macromol*. 2014;68:92–97.
35. Paul W, Sharma CP. Chitosan and alginate wound dressings: A short review. *Trends Biomater Artif Organs.* 2004;18(1):18–23.
36. Gu Z, Xie H, Huang C, Li L, Yu X. Preparation of chitosan/silk fibroin blending membrane fixed with alginate dialdehyde for wound dressing. *Int J Biol Macromol*. 2013;58:121–126.
37. Sarker B, Singh R, Silva R, et al. Evaluation of fibroblasts adhesion and proliferation on alginate-gelatin crosslinked hydrogel. *PLoS One*. 2014:9(9):e107952.
38. Pereira R, Carvalho A, Vaz DC, et al. Development of novel alginate based hydrogel films for wound healing applications. *Int J Biol Macromol*. 2013;52:221–230.
39. Thu HE, Zulfakar MH, Ng SF. Alginate based bilayer hydrocolloid films as potential slow-release modern wound dressing. *Int J Pharm*. 2012;434(1–2):375–383.
40. Goh CH, Heng PW, Huang EP, Li BK, Chan LW. Interactions of antimicrobial compounds with cross-linking agents of alginate dressings. *J Antimicrob Chemother*. 2008;62(1):105–118.
41. Shalumon KT, Anulekha KH, Nair SV, et al. Sodium alginate/poly(vinyl alcohol)/nano ZnO composite nanofibers for antibacterial wound dressings. *Int J Biol Macromol*. 2011;49(3):247–254.
42. Lee KY, Rowley JA, Eiselt P, et al. Controlling mechanical and swelling properties of alginate hydrogels independently by cross-linker type and cross-linking density. *Macromolecules*. 2000;33(11): 4291–4294.
43. Singh B, Sharma S, Dhiman A. Design of antibiotic containing hydrogel wound dressings: biomedical properties and histological study of wound healing. *Int J Pharm*. 2013;457(1):82–91.
44. P T SK, Lakshmanan VK, Raj M, et al. Evaluation of wound healing potential of β-chitin hydrogel/nano zinc oxide composite bandage. *Pharm Res.* 2013;30(2):523–537.
45. Kumar PT, Lakshmanan VK, Anilkumar TV, et al. Flexible and microporous chitosan hydrogel/nano ZnO composite bandages for wound dressing: In vitro and in vivo evaluation. *ACS Appl Mater Interfaces*. 2012;4(5):2618–2629.
46. Raghupathi KR, Koodali RT, Manna AC. Size-dependent bacterial growth inhibition and mechanism of antibacterial activity of zinc oxide nanoparticles. *Langmuir*. 2011;27(7):4020–4028.
47. Sasidharan A, Chandran P, Menon D, Raman S, Nair S, Koyakutty M. Rapid dissolution of ZnO nanocrystals in acidic cancer microenvironment leading to preferential apoptosis. *Nanoscale*. 2011;3(9): 3657–3669.
48. Venkatesan J, Bhatnagar I, Kim SK. Chitosan-Alginate Biocomposite containing fucoidan for bone tissue engineering. *Mar Drugs.* 2014; 12(1):300–316.
49. Okamotoa Y, Yanoa R, Miyatakea K, Tomohirob I, Shigemasac Y, Minamia S. Effects of chitin and chitosan on blood coagulation. *Carbohydr Polym*. 2003;53(3):337–342.

50. Holmes AR, Cannon RD, Shepherd MG. Effect of calcium ion uptake on Candida albicans morphology. *FEMS Microbiol Lett.* 1991;61(2–3): 187–193.
51. Sakai K, Koyama N, Fukuda T, et al. Search method for inhibitors of Staphyloxanthin production by methicillin-resistant *Staphylococcus aureus*. *Biol Pharm Bull*. 2012;35(1):48–53.
52. Raja A, Sivamani K, Garcia MS, Isseroff RR. Wound re-epithelialization: modulating keratinocyte migration in wound healing. *Front Biosci.* 2007;12:2849–2868.
53. Agren MS, Chvapil M, Franzén L. Enhancement of re-epithelialization with topical zinc oxide in porcine partial-thickness wounds. *J Surg Res.*1991;50(2):101–105.
54. Sharir H, Zinger A, Nevo A, Sekler I, Hershfinkel M. Zinc Released from injured cells is acting via the Zn^{2+}-sensing receptor, ZnR, to trigger signalling leading to epithelial repair. *J Biol Chem.* 2010; 285(34):26097–26106.